Zirconium Nitride Nanoparticles Prepared by Reactive Magnetron Sputtering

M. Protsak, P. Pleskunov, K. Bilia D. Nikitin, M. Tosca, and A. Choukourov
Charles University Prague, Faculty of Mathematics and Physics, Prague, Czech Republic.

Abstract. Thin films of the IV group transition-metal nitrides possess unique properties, such as chemical stability, high melting point, and hardness, and hence are widely used in industrial sectors. This work briefly introduces the field of transition-metal nitrides, in particular ZrN, and proposes their sputter-based preparation in the form of nanoparticles, which has yet been poorly studied. The first experimental results on the production of Zr and ZrN nanoparticles by DC magnetron sputtering have been obtained, and a comparison of the main characteristics of these two types of nanoparticles is presented.

Introduction

Thin films of metals and their compounds are in high demand in various fields. Of great value are those coatings that show plasmonic effects in the visible range. For a long time, the IV group transition metal nitrides (TiN, ZrN, and HfN) have been considered as plasmonic alternatives to noble metals, such as gold and silver. They significantly benefit from high hardness and melting point, chemical stability, relatively high electrical conductivity, and importantly lower price. For example, the melting temperatures of TiN, ZrN, and HfN are 2930 °C, 2980 °C, and 3330 °C, respectively, while the melting point of gold is only 1064 °C [1, 2]. Moreover, their properties can be tuned via metal/nitrogen stoichiometry. Thus, they can be used in different applications, such as optoelectronic devices [3], hot solar cells [4], decorative [5, 6], protective and anticorrosive coatings [5], in cutting tools and machining equipment [7].

To date, these transition-metal nitrides have been studied mainly in the form of thin films prepared by sputtering or other PVD techniques. However, some applications (photovoltaics, gas sensing, etc.) request a high specific area to increase the efficiency of coatings. Therefore, highly porous, three-dimensional structures (nanorods, nanotubes, and nanoparticles) are urgently needed. Few studies have explored the synthesis of nanoparticles (NPs) of transition-metal nitrides using sophisticated chemical routes; however, this area has not been investigated in depth. To our knowledge, no one has studied the sputter-based synthesis of these NPs, although our group has recently shown that this approach is feasible for the production of mesoporous coatings consisting of TaN NPs [8].

In this work, we propose using reactive DC magnetron sputtering in Ar/N_2 mixtures to produce ZrN NPs. This approach is environmentally friendly because it does not involve the use of aggressive chemical compounds, solvents, or high temperatures. Characterization is presented by comparing Zr NPs produced in Ar and ZrN NPs, obtained by sputtering in Ar/N_2. The main aim of this work is to introduce the benefits of using ZrN NP coatings as innovative plasmonic materials.

Experimental part

The production of NPs was performed using a gas aggregation cluster source (GAS) mounted onto the main vacuum chamber. Rotary and diffusion pumps were utilized to pump the deposition system down to a pressure of 10^{-3} Pa. The GAS consists of a cylindrical water-cooled chamber with a conical nozzle and a focusing orifice (diameter 4 mm, length 2 cm) at its end and is equipped with a 3-inch DC magnetron with a Zr target, which was pre-cleaned using a high current at 400 mA and low total pressure at 1.5 Pa of Ar gas for 15 min before experiments. The sputtering was performed under a fixed magnetron current at 500 mA. The Zr and ZrN NPs were obtained by sputtering in Ar and Ar/N_2 gas mixture. The flow rates of each gas were adjusted by flow controllers with the ranges of 0–20 sccm for Ar and 0–5 sccm for N_2 and accuracy 0.1 and 0.01 sccm, respectively. Under such conditions, NPs were formed in the aggregation chamber and transported to the main chamber, where the sample holder was located. The deposition rate was controlled by a movable quartz crystal microbalance (QCM) 14 mm in diameter and located at the same distance (30 cm) from the orifice as the sample holder, with a zero offset angle from the normal to the GAS orifice.

The NPs were deposited onto Si wafer or quartz substrates and analyzed using different approaches. Their size and shape were characterized by scanning electron microscopy (SEM, JSM-7200F, Jeol Ltd). All images were processed using Solarius Particles software to calculate size distributions. The chemical composition was studied using X-ray photoelectron spectroscopy (XPS, Phoibos 100, Specs), and the spectra were analyzed using the CasaXPS software. The optical absorbance measurements were performed by UV-Vis spectroscopy (Hitachi U-2900).

Results and discussion

As known for reactive sputtering of thin films, the addition of N_2 to Ar affects the sputtering process in such a way that the deposition rate significantly decreases at a certain value of the nitrogen concentration due to a poisoning effect when poorly conductive compounds are formed on the target surface [8]. Likewise, the same behavior was confirmed for the ZrN NPs, which is presented in Figure 1. Here, the sputtering was started in Ar at a flow rate set at 11.00 sccm, since the highest deposition rate of Zr NPs was obtained at this value. Then N_2 was added with 0.02 sccm increments, while Ar was proportionally decreased to keep the GAS pressure fixed at 50 Pa. After each step of adding N_2, 30 s were counted and the deposition rate was read by QCM. At low concentrations of N_2, the deposition rate stays constant or slightly increases, while it rapidly decreases when the target poisoning occurs. Moreover, the reproducibility of the deposition rate between different experiments was 20 %. The N_2 concentration immediately before poisoning was chosen as the working condition for the synthesis of ZrN NPs, as shown by a vertical dotted line in Figure 1. It was also found that the onset of poisoning changes slightly with target utilization. Therefore, the same procedure for adding N_2 was used before each of the following experiments to precisely establish the working conditions.

Zr and ZrN NPs were investigated by SEM to analyze their size and shape. Zr NPs are characterized by a faceted shape (Figures 2a,b), while the nitridation leads to the formation of NPs of irregular shape, but also cubic NPs are produced, as shown in Figures 2c,d.

The sizes were characterized by analyzing the 2489 Zr and 2388 ZrN nanoparticles from the obtained SEM images, and Figure 3 presents a comparison of the NP size distribution for these two types of material. For Zr NPs, it was well-fitted by the lognormal function with the mean size of 23 ± 4 nm (Figure 3a). However, the size distribution of ZrN NPs was fitted by a bimodal lognormal function showing two maxima at 24 and 35 nm (Figure 3b). While the size of 24 nm shows single NPs, the larger size is represented by agglomerates of smaller NPs, as can be seen from an SEM image with higher magnification (Figure 2d).

XPS measurements were performed after the samples were exposed to the ambient atmosphere to study the chemical composition. The wide spectrum of Zr NPs is characteristic of oxidized Zr (Figure 4a), as evidenced by the presence of Zr, O, and C peaks. Moreover, in addition to the main Zr

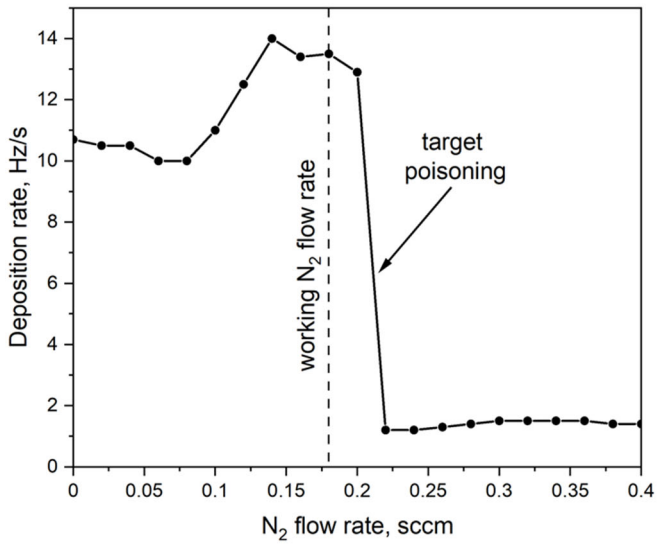

Figure 1. Deposition rate of NPs produced by reactive magnetron sputtering of Zr in Ar/N_2 mixtures as measured by QCM.

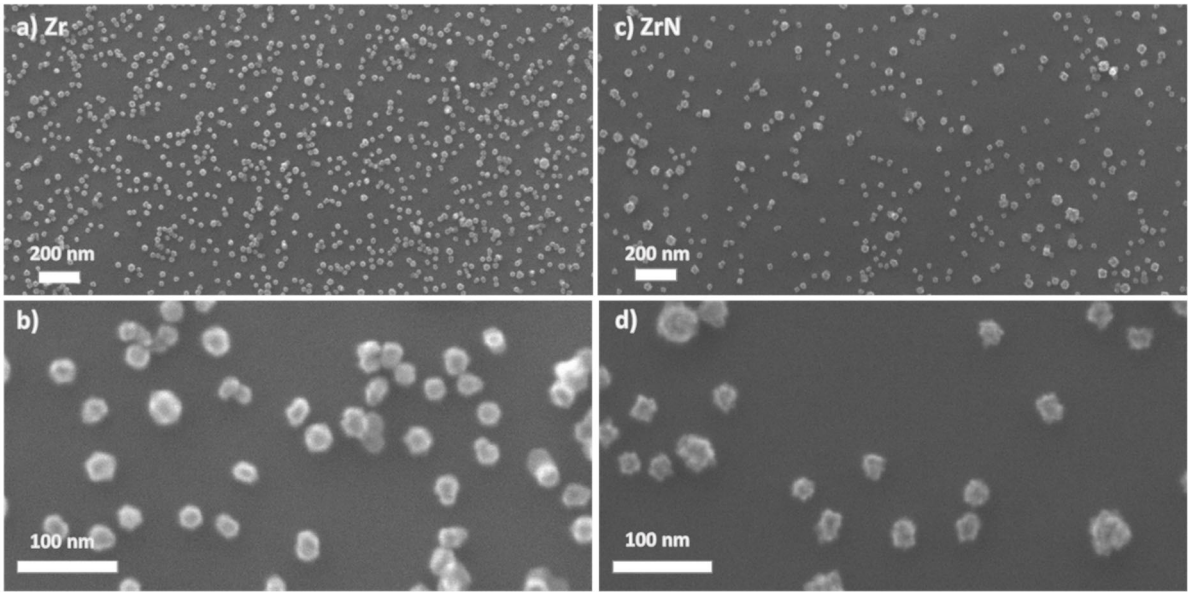

Figure 2. SEM images of two types of NPs: (a) and (b) Zr, (c) and (d) ZrN; different magnifications are shown.

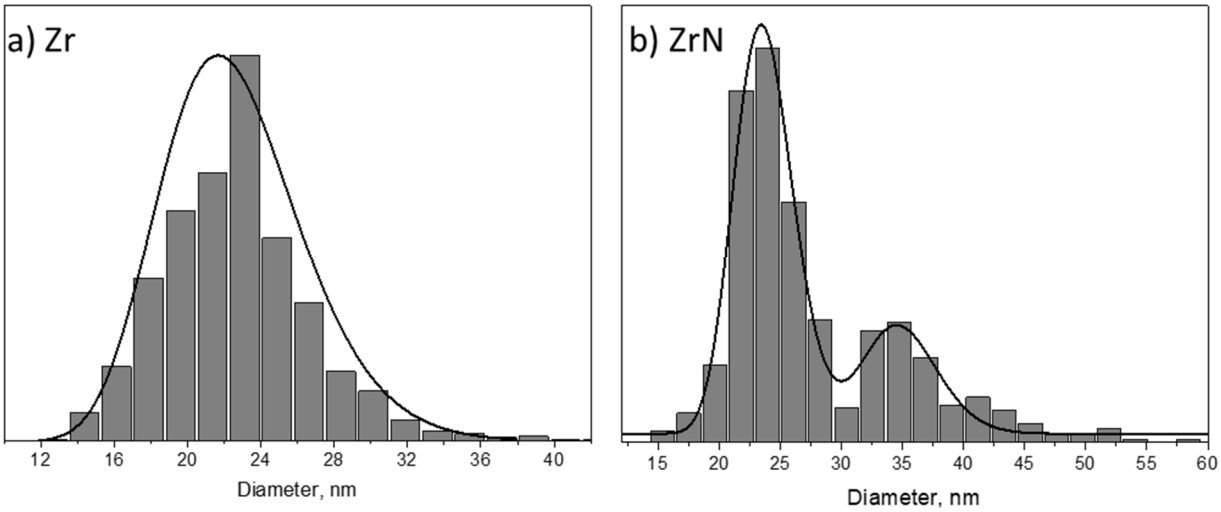

Figure 3. Comparison of NP size distribution for: (a) Zr and (b) ZrN.

3d peak, several other peaks such as Zr 3s, Zr 3p, Zr 4s, and Zr 4p were also recorded. Carbon appears in the spectrum as impurities from the air. With the addition of N_2, XPS showed the formation of NPs, which consist of Zr, N, and O (Figure 4b). The atomic composition has been calculated from these spectra and is shown in Table 1. In both cases, oxygen is incorporated as a result of the influence of the environment since metal and metal nitride NPs rapidly form oxide and oxynitride layers when exposed to the atmosphere. ZrN NPs are characterized by the N:Zr ratio of 0.52:1 (Table 1).

Optical features of both Zr and ZrN NPs were characterized by UV-Vis spectroscopy. For this purpose, such samples were deposited onto quartz substrates. It is worth noting that Zr and ZrN NPs

Table 1. Atomic compositions of Zr and ZrN NPs produced by DC magnetron sputtering as measured by XPS.

	Zr [at%]	N [at%]	O [at%]	C [at%]	N:Zr
Zr	27.0	0.0	50.1	22.9	—
ZrN	22.9	11.8	34.7	30.6	0.52:1

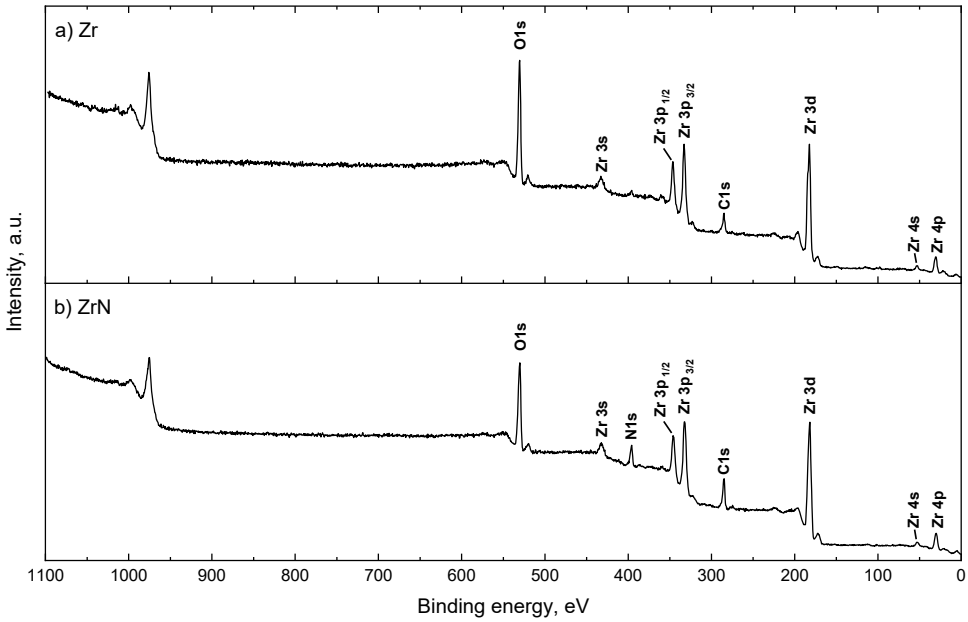

Figure 4. Comparison of wide XPS spectra of (a) Zr and (b) ZrN NPs.

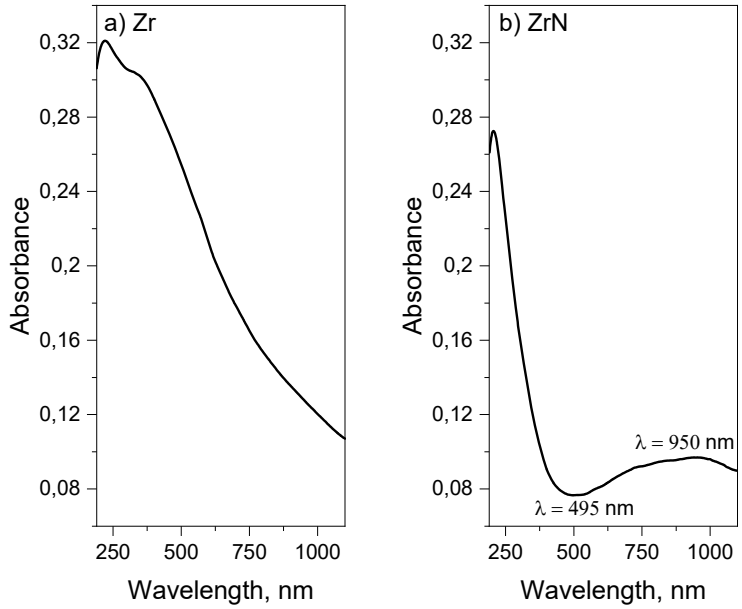

Figure 5. UV-Vis spectra measured on Zr and ZrN NPs.

appear to be brown and green-blue colored, respectively. Zr NPs sputtered in Ar absorb in the visible and near-IR range, with absorbance decreasing monotonically toward higher wavelengths (Figure 5a). Markedly, nitridation leads to changes in the optical properties. The UV-Vis spectrum of ZrN NPs (Figure 5b) shows a broad absorbance band in the red/near-IR range, with a maximum located at 950 nm. The optical absorbance in this region is responsible for the apparent green-blue color of these NPs in transmitted light. For ZrN thin films, the absorbance maximum in this region is often attributed to Localized Surface Plasmon Resonance (LSPR). Currently, we are not able to definitely establish whether LSPR is responsible for the optical absorbance in the ZrN NPs, and additional experiments must be performed in the future.

Conclusions

In this work, perspectives on the synthesis of transition-metal nitride NPs were discussed and found to be very promising. From an experimental point of view, the work is dedicated to producing and

characterizing ZrN NPs. ZrN NPs were successfully prepared by reactive magnetron sputtering in Ar/N_2 mixtures using GAS. They were compared to Zr NPs produced in the same way but using Ar as the working gas. Thereby, the influence of nitridation was investigated. ZrN NPs are characterized by a mean size of 24 nm, an N:Zr ratio of 0.52:1, and a characteristic optical absorbance in the red/near-IR range, which hypothetically can originate from localized surface plasmon resonance. The first experiments did not reach the stoichiometric composition; therefore, further studies have been planned to provide detailed research and improve the experimental approach.

Acknowledgments. The work was supported via the grant GACR 21-12828S from the Czech Science Foundation; the Charles University Grant Agency under Contract 372322; M.P, K.B., and M.T. also appreciate the support from the Charles University via a student grant SVV 260 579-2021.

References

[1] A. Lalisse, G. Tessier, J. Plain, and G. Baffou, "Plasmonic efficiencies of nanoparticles made of metal nitrides (TiN, ZrN) compared with gold," *Scientific Reports*, vol. 6, Dec. 2016, doi: 10.1038/srep38647.

[2] Y. Zhong, X. H. Xia, F. Shi, J. Y. Zhan, J. P. Tu, and H. J. Fan, "Transition metal carbides and nitrides in energy storage and conversion," *Advanced Science*, vol. 3, no. 5. Wiley-VCH Verlag, Jan. 01, 2015. doi: 10.1002/advs.201500286.

[3] D. I. Bazhanov, A. A. Knizhnik, A. A. Safonov, A. A. Bagatur'yants, M. W. Stoker, and A. A. Korkin, "Structure and electronic properties of zirconium and hafnium nitrides and oxynitrides," *Journal of Applied Physics*, vol. 97, no. 4, Feb. 2005, doi: 10.1063/1.1851000.

[4] S. Chung *et al.*, "Hafnium nitride for hot carrier solar cells," *Solar Energy Materials and Solar Cells*, vol. 144, pp. 781–786, Jan. 2016, doi: 10.1016/j.solmat.2014.10.011.

[5] E. Budke, J. Krempel-Hesse, H. Maidhof, and H. Schüssler, "Decorative hard coatings with improved corrosion resistance," *Surface and Coatings Technology*, vol. 112, no. 1–3, pp. 108–113, Feb. 1999, doi: 10.1016/S0257-8972(98)00791-9.

[6] S. Niyomsoan, W. Grant, D. L. Olson, and B. Mishra, "Variation of color in titanium and zirconium nitride decorative thin films," *Thin Solid Films*, vol. 415, no. 1–2, pp. 187–194, Aug. 2002, doi: 10.1016/S0040-6090(02)00530-8.

[7] J. M. Molarius, A. S. Korhonen, E. Harju, and R. Lappalainen, "Comparison of cutting performance of ion-plated NbN, ZrN, TiN and (Ti, Al)N coatings," *Surface and Coatings Technology*, vol. 33, no. C, pp. 117–132, 1987, doi: 10.1016/0257-8972(87)90182-4.

[8] P. Pleskunov *et al.*, "The sputter-based synthesis of tantalum oxynitride nanoparticles with architecture and bandgap controlled by design," *Applied Surface Science*, vol. 559, Sep. 2021, doi: 10.1016/j.apsusc.2021.149974.